# Furin-mediated processing in the early secretory pathway: Sequential cleavage and degradation of misfolded insulin receptors

**Joseph Bass*†‡, Christopher Turck§, Mathias Rouard*¶, and Donald F. Steiner*†‖**

*Howard Hughes Medical Institute and Departments of ‖Biochemistry and Molecular Biology and †Medicine, The University of Chicago, Chicago, IL 60637; and §Department of Medicine, Cardiovascular Research Institute, and Howard Hughes Medical Institute, University of California, San Francisco, CA 94143

Contributed by Donald F. Steiner, August 17, 2000

**Improperly folded membrane proteins are retained in the endoplasmic reticulum and then diverted to a degradative pathway by a network of molecular chaperones and intracellular proteases. Here we report that mutant insulin proreceptors ($Pro^{62}$) retained in the early secretory pathway undergo proteolytic cleavage at a tetrabasic concensus site for the subtilisin-like protease furin (SPC 1), generating two unstable proteolytic intermediates of 80/120 kDa corresponding to $\alpha$ (135 kDa) and $\beta$ (90 kDa) subunits. These are degraded more rapidly than the uncleaved proreceptor protein. Site-directed mutagenesis of the normal RKRR processing site prevented cleavage. Use of inhibitors and furin-deficient cell lines confirmed that furin is responsible for proreceptor cleavage; furin overexpression increased the degradation of mutant but not wild-type receptors. Together, these results suggest that processing and degradation occur sequentially for mutant proreceptors.**

biosynthesis | calnexin | calreticulin | degradation | endoplasmic reticulum

A central question in cell biology is how do eukaryotic cells distinguish and eliminate improperly folded proteins from the secretory pathway, a process referred to as biosynthetic quality control. Recent evidence indicates that degradation occurs after translocation from the endoplasmic reticulum (ER) to the cytosol and involves the 26S proteasome (1–11). However, the mechanism by which integral membrane proteins might be extruded from the ER remains unclear. Pharmacologic studies are beginning to support a role for proteases in biosynthetic quality control, including those with both trypsin and chymotrypsin-like activities, metalloproteinases, and the signal peptidase (12–17).

Missense mutations in the insulin receptor (IR) that cause diabetes mellitus provide an example of a protein folding disorder in which cells recognize and destroy the abnormal protein (18–20). Studies of the biosynthesis of the wild-type IR have revealed that it initially is synthesized as a single chain proreceptor, which slowly folds and dimerizes in the ER and then is transported to the trans-Golgi where it is cleaved into two $\alpha$ and two $\beta$ subunits (21, 22). The mature subunits acquire sialic acid before transport to the cell surface (21–25). Misfolded receptors diverge from this pathway and are instead retained in the ER.

We previously found that two proteins of 120 and 80 kDa accumulated in cells producing mutant receptors (26). Here we show that the 120- and 80-kDa proteins are immunoreactive with antireceptor antibodies, and they are generated by cleavage of the proreceptor. However, the 120- and 80-kDa proteins retain immature carbohydrates characteristic of localization in the ER or cis-Golgi. Radiosequencing revealed that cleavage of the proreceptor into 120/80-kDa proteins occurs at a concensus site for the subtilisin-like protease, furin (RKRR ↓ ), an unexpected finding because furin was thought to act primarily in the trans-Golgi network (TGN). Together with recent work on the cleavage of the sterol regulatory element binding protein (27, 28), the studies here suggest that pro-protein processing by the subtilisin-like pro-protein convertases can occur without transport of the substrate to the cell surface. The experiments also suggest that furin cleavage depends on substrate conformation, a finding that may be relevant to other misfolded proteins that are processed by furin.

## Materials and Methods

**General Materials and Methods.** Restriction enzymes and other reagents were molecular biology grade. mAb 83–14 was a gift from K. Siddle (Addenbrooke's Hospital, University of Cambridge, Cambridge, U.K.) (29), anticalnexin (anticalnexin and antiubiquitin antibodies) was from StressGen Biotechnologies, Victoria, Canada, and anticalreticulin was from Affinity Bioreagents (Golden, CO).

**Mutagenesis, Cell Lines, and Transfections.** Expression plasmids containing mutant and wild-type IRs were prepared as described (26). Site-directed mutagenesis was conducted by using QuickChange (Stratagene). The forward/reverse strand primers were 5′-CCTAGGCCATCTGCGAAACGCAGGTCC-3′/5′-GGACCTGCGTTTCGCAGATGGCCTAGG-3′ for mutagenesis of R732A in pcDNA3.1 containing the $Pro^{62}$-IR cDNA (the mutated nucleotides are underlined). Mutagenesis was confirmed by cycle sequencing (Perkin–Elmer). Stable HEK293 cell lines expressing $Pro^{62}$ receptors were maintained as described (26), and isogenic cell lines expressing the wild-type receptor were a gift of Jonathan Whittaker (Hagedorn Research Institute, Gentofte, Denmark). Transient transfections were performed by using Lipofectamine (Life Technologies, Gaithersburg, MD). CHO-K1 and RPE.40 cells (provided by Thomas Moehring, University of Vermont, Burlington) were grown in Ham's F-12 medium with 5% FCS, 100 units/ml penicillin, and 100 $\mu$g/ml streptomycin. Furin cDNA was provided by Steve Duguay (Transkaryotic Therapies, Cambridge, MA).

**Metabolic Labeling and Sucrose Density Gradient Analysis.** Metabolic labeling, immunoprecipitation, and immunoblotting was performed as described (25, 26). For 5–30% sucrose density gradient analysis, cell extracts prepared in 2% CHAPS (3-[(3-cholamidopropyl)dimethylammonio]-1-propanesulfonate), 200 mM NaCl, 50 mM Hepes, and gradients were centrifuged in a Beckman SW 50.1 rotor at 40,000 rpm to $\omega^2t = 9.0 \times 10^{11}$ (14.25 h). Gradient fractions were immunoprecipitated with antirecep-

Abbreviations: ER, endoplasmic reticulum; IR, insulin receptor; BFA, brefeldin A; endo H, endoglycosidase H; TGN, trans-Golgi network.

‡To whom reprint requests should be sent at present address: Northwestern University Medical School and the Evanston Northwestern Healthcare Research Institute, 1033 University Place, Suite 420, Evanston, IL 60201. E-mail: j-bass@northwestern.edu.

¶Present address: Wellcome Trust Centre for Human Genetics, Roosevelt Drive, Headington, Oxford OX3 7BN, United Kingdom.

The publication costs of this article were defrayed in part by page charge payment. This article must therefore be hereby marked "*advertisement*" in accordance with 18 U.S.C. §1734 solely to indicate this fact.

tor antibodies and processed for 3–10% linear gradient SDS/PAGE (25, 30). For incubation with BFA, cells were incubated for 15–30 min in cold labeling medium with 5 $\mu$g/ml brefeldin A (BFA), then pulse-labeled with 100 $\mu$Ci/ml of [$^{35}$S]cysteine and [$^{35}$S]methionine, and chased in medium containing excess cysteine and methionine and 5 $\mu$g/ml BFA. Control incubations were in DMSO without BFA (final 0.5% vol/vol).

**Glycosidase Digestion.** Samples were processed for glycosidase digestion with endoglycosidase H (endo H) and neuraminidase as described (25).

**Radiosequencing.** Cells were labeled overnight with [$^{3}$H]leucine, [$^{3}$H]tyrosine, or [$^{3}$H]valine, and lysed, and receptors were immunoprecipitated and processed for gel electrophoresis. After electrophoresis, gels were transferred to Immobilon Sequencing Membrane (Millipore) in CAPS [3-(cyclohexylamino)-1-propanesulfonic acid] buffer (50 mM CAPS, pH 9.9/20% methanol) and stained with Coomassie brilliant blue. Poly(vinylidene difluoride) membrane pieces that contained the protein were subjected to radioactive Edman degradation in a blot cartridge on an Applied Biosystems model 492 sequencer (Perkin–Elmer). After each cycle, the cleaved ATZ amino acids were extracted by three 15-s treatments with ethyl acetate. The ATZ-amino acid extracts were collected into a 5-ml scintillation tube, and the solvent was evaporated overnight. Scintillation fluid was added to the tube and counted for 1 min in a Beckman Scintillation Counter.

## Results

**Misfolding and Misprocessing of Mutant Receptors.** Pro$^{62}$ IRs were previously identified in a young woman with clinical insulin resistance, and expression in heterologous cell lines showed that the mutant receptors were degraded intracellularly (26). To compare the maturation of wild-type and mutant receptors we used sucrose density gradient analysis. Four maturation intermediates were found during biosynthesis of the wild-type receptor in HEK293 cells, including two monomer isoforms (early and late monomers), the dimer, and tetramer (Fig. 1*A*). However, the Pro$^{62}$ IR was only present as the monomer (fractions 9–11) (Fig. 1*A*).

Processing of mutant and wild-type receptors was analyzed by reducing gel electrophoresis. At 2 h of chase, 90% of the wild-type Pro-IR (≈200 kDa) was processed to mature $\alpha$ (≈130 kDa) and $\beta$ (≈90 kDa) subunits. Interestingly, at early time points, ≈10% of the wild-type IR was processed to proteins of 120 and 80 kDa (Fig. 1*B*). The appearance of the 120/80-kDa proteins during the biosynthesis of the wild-type receptor was previously observed in studies of adipose cell lines (31). Because folding and transport of the wild-type receptor is ≈90% efficient, it is likely that the 120/80-kDa proteins represent 10% of newly synthesized proreceptor, which is eliminated from the cell.

In cell lines producing the Pro$^{62}$ pro-IR, the mature $\alpha$ and $\beta$ subunits did not appear at later chase time points; however, the proreceptor was processed to two proteins of 120/80 kDa and these proteins gradually increased with chase (Fig. 1*B*). Because very little of the 120- and 80-kDa proteins were detected immediately after a 5-min pulse labeling (Fig. 1*B*), it is unlikely that they were a consequence of proteolysis occurring after cell lysis.

To examine the half-lives of the proreceptor and the 120/80-kDa proteins, we used cycloheximide chase (Fig. 1*C*). After 4 h of incubation in cycloheximide, more than 50% of the 80-kDa protein disappeared from the cell, indicating that it had a much shorter half-life than that of the uncleaved proreceptor (Fig. 1*C*). The half-life of the 120-kDa protein was the same of that of the 80-kDa protein (data not shown). In cells expressing the wild-type receptor, the proreceptor was not usually detected in 100 $\mu$g of lysate protein. Similar results were obtained by metabolic labeling and corresponded with reports from other laboratories on the kinetics of mutant receptor degradation (19). These results indicate that the 80-kDa protein was less stable than the full-length proreceptor.

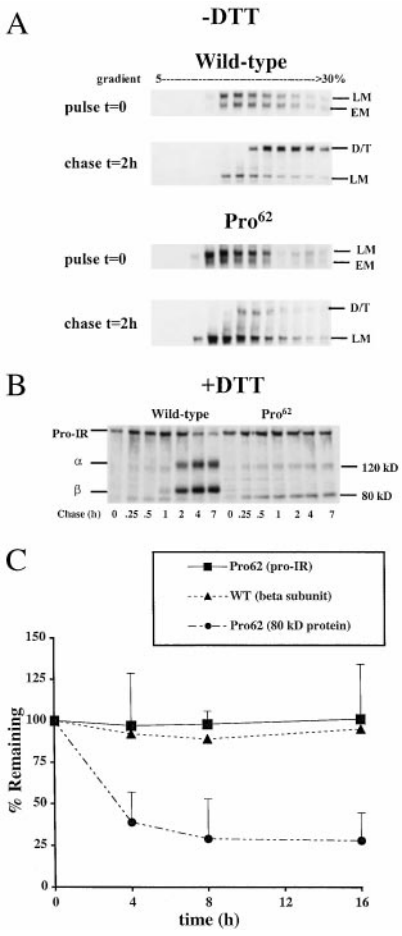


**Fig. 1.** Misprocessing of mutant IRs. (*A*) Sucrose density gradient analysis of receptor dimerization. Cells expressing wild-type and Pro$^{62}$ IR (Pro-IR) were pulse-labeled for 30 min, chased for 2 h, then separated by 5–30% sucrose density gradient. Each gradient fraction was immunoprecipitated with anti-receptor antibodies and analyzed by gel electrophoresis. The positions of the folding intermediates are indicated (EM, early monomer; LM, late monomer; D, dimer; T, tetramer). (*B*) Reducing gel analysis after a 5-min pulse (Pro-IR; $\alpha$ subunit, $\alpha$; $\beta$ subunit, $\beta$; 120-kDa and 80-kDa bands). (*C*) Cycloheximide chase. Cells were incubated in cycloheximide, and then cell lysates were processed for immunoblotting with anti-$\beta$ subunit antibodies at the indicated times. Equivalent amounts of cell lysate protein were analyzed at each time point and the data are represented as the percentage of each subunit present at the beginning of the incubation period ($t$ = 0). Pro-IR, Pro$^{62}$ proreceptor, 80-kDa protein; WT ($\beta$ subunit), wild-type IR $\beta$ subunit. Each point represents data from four separate experiments.

**The 120/80-kDa Proteins Have Immature Glycans and Are Generated in the Presence of BFA.** To determine the subcellular localization of the 120/80-kDa proteins, we examined the effect of endo H digestion on the gel mobility of the 120/80-kDa fragments (reviewed in ref. 32). We found that endo H digestion caused a gel shift of the proreceptor of ≈30 kDa, the 120-kDa protein of ≈28 kDa, and the 80-kDa protein of ≈8 kDa, consistent with high mannose N-linked glycans at 14 sites in the $\alpha$ subunit and three sites in the $\beta$ subunit (Fig. 2*A*, lanes 1 and 5). After 7 h

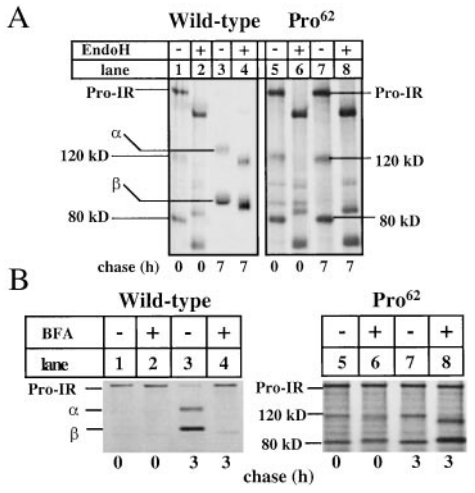


**Fig. 2.** Localization of proreceptor processing analyzed with endo H and BFA. (*A*) HEK293 cells expressing wild-type and Pro$^{62}$ receptors were pulse-labeled for 15 min and then extracts were prepared after the pulse and 7 h of chase, immunoprecipitated, and then incubated with buffer alone (control) or endo H. The positions of receptor subunits and 120/80-kDa bands are indicated. (*B*) Pulse–chase labeling performed in the presence or absence of 5 $\mu$g/ml BFA.

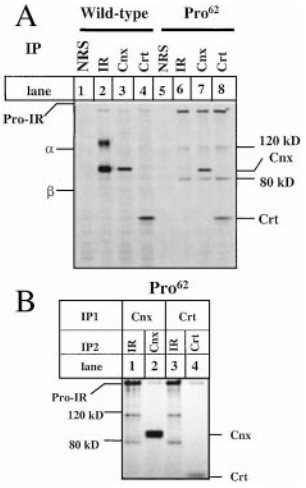


**Fig. 3.** Complexes with ER chaperones. (*A*) HEK293 cells expressing wild-type and Pro$^{62}$ IR were pulse–chase-labeled and lysed in CHAPS (3-[(3-cholamidopropyl)dimethylammonio]-1-propanesulfonate). Samples were divided equally for immunoprecipitation with calnexin (Cnx) and calreticulin (Crt), and one-half equivalent volume was immunoprecipitated with receptor antibodies and then processed for 5/8% SDS/PAGE. The antibody used for the immunoprecipitation is indicated at the top. NRS, nonimmune rabbit serum. (*B*) Sequential IP with antichaperone and antireceptor antibodies.

chase, most of the wild-type pro-IR was converted to the $\alpha/\beta$ subunits and acquired endo H resistance (Fig. 2*A*, lanes 3 and 4 vs. 1 and 2), in contrast, after chase, the Pro$^{62}$ receptor was still fully endo H-sensitive (Fig. 2*A*, lanes 7 and 8). Because of the long labeling period, and the slow conversion of the pro-IR to the 120/80-kDa proteins, the ratio of Pro$^{62}$ pro-IR to 120/80-kDa proteins was similar at the pulse and chase time points. The sensitivity of the 120/80-kDa proteins to endo H suggests that these proteins did not reach the TGN.

We took a second approach to examine the subcellular localization of the proreceptor and 120/80-kDa proteins, using BFA, which causes the redistribution of enzymes in the TGN to the ER (Fig. 2*B*) (33). As expected, processing of the wild-type receptor into $\alpha$ and $\beta$ subunits was inhibited by BFA (Fig. 2*B*, lanes 3 and 4) (30, 31). However, BFA did not decrease processing of the Pro$^{62}$ insulin proreceptor to 120/80 kDa (Fig. 2*B*, lanes 7 and 8). The altered electrophoretic mobility of the proreceptor and 120/80-kDa proteins in the presence of BFA was caused by changes in carbohydrate modification associated with the admixture of carbohydrate-modifying enzymes in the ER with those in the cis- and medial-Golgi (data not shown). The results of both endo H digestion and BFA treatment indicate that the wild-type and Pro$^{62}$ proreceptors are processed in different subcellular compartments.

**ER Molecular Chaperones Bind to Cleaved Mutant Receptors.** To monitor the progress of the receptor through the ER, we examined complexes between ER molecular chaperones and the full-length and processed receptor (25) (Fig. 3*A*, lane 2). Cells were pulse-labeled and lysed in CHAPS (3-[(3-cholamidopropyl)dimethylammonio]-1-propanesulfonate) followed by sequential immunoprecipitation with antichaperone and antireceptor antibodies (Fig. 3). The identity of each protein in complexes with calnexin and calreticulin was confirmed by sequential immunoprecipitation and immunoblotting (data not shown). Twice as much cell lysate protein was used for antichaperone immunoprecipitations to facilitate detection of the proteins associated with calnexin/calreticulin (Fig. 3*A*). In agreement with previous studies, the mature $\alpha$ and $\beta$ subunits were not recovered by immunoprecipitation with anticalnexin or anticalreticulin antibodies (Fig. 3*A*, lanes 3 and 4). In control immunoprecipitation with nonimmune serum there was no binding of the 120/80-kDa proteins (Fig. 3*A*, lanes 1 and 5). The Pro$^{62}$ pro-IR was still the predominant species of receptor in the cell at 7 h chase, with partial conversion to the 120/80-kDa fragments (Fig. 3*A*, lane 6). Moreover, the Pro$^{62}$ pro-IR and 120/80-kDa fragments were coimmunoprecipitated with antibodies to calnexin and calreticulin (Fig. 3*A*, lanes 7 and 8; Fig. 3*B*, lanes 1 and 3). The results indicate either that cleavage of the Pro$^{62}$ pro-IR does not involve transport to the trans-Golgi, or that after cleavage, the 120/80-kDa proteins undergo retrograde transport from the Golgi to the ER.

**Location of the Processing Site in the Pro$^{62}$ Insulin Proreceptor.** To identify the 120/80-kDa proteins, we isolated and sequenced each protein. Cells expressing the mutant Pro$^{62}$ IR were used for isolation of the 120/80-kDa proteins because no mature $\alpha$ or $\beta$ subunits were present. These cells were pulse-labeled with [$^3$H]leucine, [$^3$H]tyrosine, or [$^3$H]valine. Then, the 120- and 80-kDa proteins were isolated after immunoprecipitation, gel electrophoresis, and transfer to Immobilon-P$^{SQ}$ membrane (Fig. 4). Based on radio sequencing, the identity of the N-terminal amino acid residue of both the 120- and 80-kDa proteins was determined. Tyrosine, valine, and leucine occur in a unique sequence after Ser-736, indicating that the amino terminus of the 80-kDa protein was located at this residue (Fig. 4*B*). These data were confirmed by direct sequencing of the 80-kDa fragment. The occurrence of valine and leucine in radio sequencing of the 120-kDa fragment corresponded to the unique primary sequence at residue 1 of the $\alpha$ subunit (Fig. 4*A*) (22, 23). The sequence immediately preceding Ser-736 contains a canonical furin site including an arginine in the P4 position (RKRR $\downarrow$). The radio sequencing data show that the 120/80-kDa proteins are derived from proteolytic cleavage of the full-length pro-IR between Arg-735–Ser-736.

**Furin Is Responsible for Cleavage of the Malfolded Receptors.** To determine whether furin mediates cleavage of the proreceptor into the 120/80-kDa proteins we first expressed the wild-type and Pro$^{62}$ receptors in a furin-deficient Chinese hamster ovary

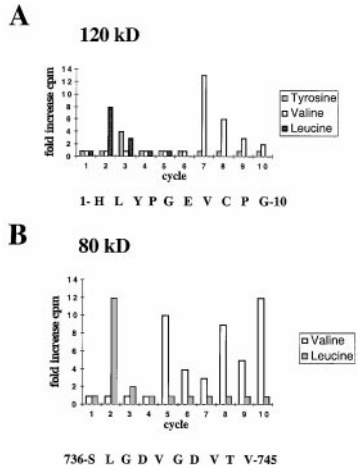


**Fig. 4.** Identification of the $Pro^{62}$ Pro-IR processing site by radio sequencing. HEK293 cells expressing $Pro^{62}$ receptors were metabolically labeled, then immunoprecipitated and processed for gel electrophoresis. cpms in the eluted fractions are shown, and each point represents the mean from at least three separate experiments expressed as the fold-increase over baseline. The receptor sequence is shown below in single-letter amino acid codes. (*A*) Radio sequencing of the 120-kDa protein and (*B*) the 80-kDa protein.

cell line (Fig. 5*A*) (34). In these experiments, levels of endogenous IR were below the limit of detection. In furin-deficient cell lines, processing of the wild-type receptor was reduced by ≈50%; however, the unprocessed pro-IR still progressed to the TGN and acquired complex glycans (25). These results could be explained by the presence of other prohormone convertases in the furin-deficient cells that could contribute to the cleavage of the pro-IR (35). Processing of the $Pro^{62}$ IR was nearly undetectable in the furin-deficient cell line.

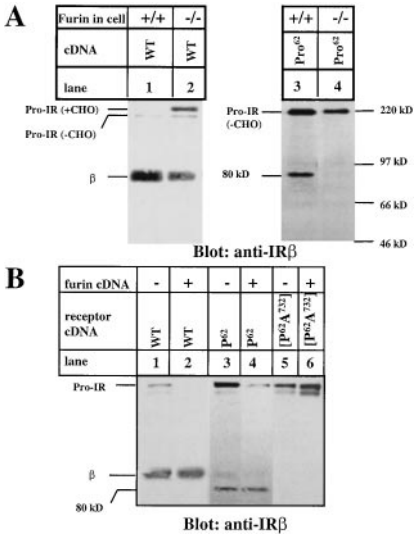


**Fig. 5.** Requirement for furin in proreceptor proteolytic processing. Immunoblot analysis of receptors transfected into furin-null RPE40 cells and the isogenic control cells (furin+). The presence of carbohydrate added in the trans-Golgi is indicated (added carbohydrate, +CHO; without added carbohydrate, −CHO). Exposure times of the ECL film for wild-type (WT) and $Pro^{62}$ samples were optimized separately. (*B*) Immunoblot analysis of receptors transfected into HEK293 cells. The transfected cDNA is indicated at the top (lane 1, WT; lane 2, WT and furin; lane 3, $Pro^{62}$ ($P^{62}$); lane 4, $Pro^{62}$ and furin; lane 5, $[P^{62}A^{732}]$; lane 6, $[P^{62}A^{732}]$ and furin).

To examine the effect of furin on the degradation of $Pro^{62}$ IR, we cotransfected cDNAs for furin and the receptor in HEK293 cells. Coexpression of furin with $Pro^{62}$ IR cDNA increased receptor degradation by 85% in three separate experiments (Fig. 5*B*, lanes 3 and 4). In contrast, furin did not reduce the concentration of the wild-type receptor (Fig. 5*B*, lanes 1 and 2).

In a second approach to confirm whether furin was responsible for cleavage of the $Pro^{62}$ IR, we substituted the conserved P4 position in the tetrabasic cleavage site of the $Pro^{62}$ receptor $[P^{62}A^{732}]$ (25). Fig. 4*B*, lane 5, shows that substitution of the P4 arginine with alanine in the $Pro^{62}$ receptor prevents processing to the 80-kDa protein. Notably, cotransfection of furin with the $[P^{62}A^{732}]$ receptor did not induce degradation (Fig. 5*B*, lanes 5 and 6 versus lanes 3 and 4). We also performed experiments with the potent chloromethylketone furin inhibitor (RVKR-CMK) and found reduced cleavage of $Pro^{62}$ receptors (data not shown) (36).

## Discussion

Many proteins initially are synthesized as inactive precursors requiring cleavage by furin in the constitutive secretory pathway for biologic activity. These include the Notch receptor, HIV gp160, and β nerve growth factor (37). The major finding in the present study is that furin cleavage also can occur without transport of a proprotein to the TGN. An altered proprotein conformation confers furin susceptibility in a pre-TGN compartment. Three potential mechanisms could explain our findings: (*i*) the furin cleavage site is unmasked and exposed to furin in the mutant protein, (*ii*) the improperly folded proprotein complexes with a furin inhibitor, or (*iii*) the misfolded proprotein causes the intracellular redistribution of furin.

Previous studies have demonstrated that processing of wild-type insulin proreceptors into α and β subunits occurs only in the TGN (25, 37–39). Moreover, it is well established that furin is only active after autocatalytic removal of the prodomain. Although prodomain cleavage occurs in the ER, the prodomain is thought to remain associated and act as an inhibitor until it dissociates in the TGN. The discrepancy between the present report that processed IRs are present in the ER, and the wealth of data showing that furin is active in the TGN, could be explained if the presence of unfolded protein caused the redistribution of active furin to the cis-Golgi or ER. Precedent for a recycling pathway can be found in studies on viral membrane proteins (40). Alternatively, the mutant receptor could displace the inhibitory pro segment (37).

Studies on another misfolded furin substrate, the Abri propeptide, are concordant with our finding that furin-mediated cleavage is sensitive to the physical conformation of the substrate (41). An intriguing observation was more recently reported in studies of macrophage inhibitory cytokine (MIC-1), demonstrating that the prodomain of this furin substrate is involved in targeting misfolded variants to the ubiquitin-proteasome pathway (42). A degradation signal might colocalize with the furin cleavage site and explain the requirement for an intact proprotein in the degradation of the MIC proprotein. It is possible that unmasking of the furin-cleavage site in the insulin proreceptor similarly corresponds with exposure of a degradation motif. Further analysis of the subcellular trafficking of mutant proproteins might reveal whether furin-mediated cleavage occurs directly in the lumen of the ER or in a compartment of the cis- or medial-Golgi. Furin or proreceptor recycling might involve molecular ''sorters,'' or altered phophorylation implicated in the subcellular trafficking of furin (39).

The reduced half-life of the cleaved proreceptor together with increased degradation with furin overexpression indicate that furin is rate-limiting in this process. It has been well established that mutant proteins undergo retrotranslocation from the ER and then

undergo proteasomal degradation in the cytoplasm (5–10). Previous studies have shown that mutant IRs are degraded by the proteasome; it is therefore possible that furin-mediated cleavage precedes retrotranslocation and proteasomal degradation.

We thank M. Milewski for technical assistance. We also thank Graeme Bell, Steve Duguay, Ed Fisher, Bill Green, Mark Hochstrasser, Rick Morimoto, and Gene Webb for helpful discussions and comments on the manuscript. We thank Rosie Ricks for her expert assistance in the preparation of this manuscript. This study was supported by a National Institutes of Health Career Development Award to J.B. (KO8DK02675), by National Institutes of Health Grants (D.F.S.) DK13914 and DK20595, and by the Howard Hughes Medical Institute.

1. Sommer, T. & Jentsch, S. (1993) *Nature (London)* **365,** 176–179.
2. Ward, C. L., Omura, S. & Kopito, R. R. (1995) *Cell* **83,** 121–127.
3. Jensen, T. J., Loo, M. A., Pind, S., Williams, D. B., Goldberg, A. L. & Riordan, J. R. (1995) *Cell* **83,** 129–135.
4. Hammond, C. & Helenius, A. (1995) *Curr. Opin. Cell Biol.* **7,** 523–529.
5. Werner, E. D., Brodsky, J. L. & McCracken, A. A. (1996) *Proc. Natl. Acad. Sci. USA* **93,** 13797–13801.
6. Wiertz, E. J. H. J., Tortorella, D., Bogyo, M., Yu, J., Mothes, W., Jones, T. R., Rapoport, T. A. & Ploegh, H. L. (1996) *Nature (London)* **384,** 432–437.
7. Qu, D., Teckman, J. H., Omura, S. & Perlmutter, D. H. (1996) *J. Biol. Chem.* **271,** 22791–22795.
8. Plemper, R. K., Bohmler, S., Bordallo, J., Sommer, T. & Wolf, D. H. (1997) *Nature (London)* **388,** 891–895.
9. Brodsky, J. L. & McCracken, A. A. (1997) *Trends Cell Biol.* **7,** 151–156.
10. Bordallo, J., Plemper, R. K., Finger, A. & Wolf, D. H. (1998) *Mol. Biol. Cell* **9,** 209–222.
11. Kim, P. S. & Arvan, P. (1998) *Endocr. Rev.* **19,** 173–202.
12. Wikstrom, L. & Lodish, H. L. (1991) *J. Cell Biol.* **113,** 997–1007.
13. Gardner, A. M., Aviel, S. & Argon, Y. (1993) *J. Biol. Chem.* **268,** 25940–25947.
14. Otsu, M., Urade, R., Kito, M., Omura, F. & Kikuchi, M. (1995) *J. Biol. Chem.* **270,** 14958–14961.
15. Kumar, N. M. & Gilula, N. B. (1996) *Cell* **84,** 381–388.
16. Vecchi, M. & Carpenter, G. (1997) *J. Cell Biol.* **139,** 995–1003.
17. Urade, R., Takenaka, Y. & Kito, M. (1993) *J. Biol. Chem.* **268,** 22004–22009.
18. Kahn, C. R., Flier, J. S., Bar, R. S., Archer, J. A., Gorden, P., Martin, M. M. & Roth, J. (1976) *N. Engl. J. Med.* **294,** 739–745.
19. Imamura, T., Haruta, T., Takata, Y., Usui, I., Iwata, M., Ishihara, H., Ishiki, M., Ishibashi, O., Ueno, E., Sasaoka, T., *et al.* (1998) *J. Biol. Chem.* **273,** 11183–11188.
20. Taylor, S. I., Wertheimer, E., Accili, D., Cama, A., Hone, J., Roach, P., Quon, M. J., Suzuki, Y., Levy-Toledano, R., Taouis, M., *et al.* (1994) *Endocr. Rev.* **2,** 58–65.
21. Kasuga, M., Hedo, J. A., Yamada, K. M. & Kahn, C. R. (1982) *J. Biol. Chem.* **257,** 10392–10399.
22. Ebina, Y., Ellis, L., Jarnagin, K., Edery, M., Graf, L., Clauser, E., Ou, J. H., Masiarz, F., Kan, Y. W., Goldfine, I. D., *et al.* (1985) *Cell* **40,** 747–758.
23. Ullrich, A., Bell, J. R., Chen E. Y., Herrera, R., Petruzzelli, L. M., Dull, T. J., Gray, A., Coussens, L., Liao, Y. C., Tsubokawa, M., *et al.* (1985) *Nature (London)* **313,** 756–761.
24. Olson, T. S., Bamberger, M. J. & Lane, M. D. (1988) *J. Biol. Chem.* **263,** 7342–7351.
25. Bass, J., Chiu, G., Argon, Y. & Steiner, D. F. (1998) *J. Cell Biol.* **141,** 637–646.
26. Rouard, M., Bass, J., Grigorescu, F., Garrett, T. P., Ward, C. W., Lipkind, G., Jaffiole, C., Steiner, D. F., Bell, G. I., *et al.* (1999) *J. Biol. Chem.* **274,** 18487–18491.
27. Brown, M. S. & Goldstein, J. L. (1999) *Proc. Natl. Acad. Sci. USA* **96,** 11041–11048.
28. DeBose-Boyd, R. A., Brown, M. S., Li, W. P., Nohturfft, A., Goldstein, J. L. & Espenshade, P. J. (1999) *Cell* **99,** 703–712.
29. Prigent, S. A., Stanley, K. K. & Siddle, K. (1990) *J. Biol. Chem.* **265,** 9970–9977.
30. Millar, N. S., Moss, S. J. & Green, W. N. (1995) in *Ion Channels*, ed. Ashley, R. H. (Oxford Univ. Press, New York), pp. 191–217.
31. Ronnett, G. V., Knutson, V. P., Kohanski, R. A., Simpson, T. L. & Lane, M. D. (1984) *J. Biol. Chem.* **259,** 4566–4575.
32. Kornfeld, R. & Kornfeld, S. (1985) *Annu. Rev. Biochem.* **54,** 631–664.
33. Klausner, R. D., Donaldson, J. G. & Lippincott-Schwartz, J. (1992) *J. Cell Biol.* **116,** 1071–1080.
34. Robertson, B. J., Moehring, J. M. & Moehring, T. J. (1993) *J. Biol. Chem.* **268,** 24274–24277.
35. Duguay, S. J., Milewski, W. M., Young, B. D., Nakayama, K. & Steiner, D. F. (1997) *J. Biol. Chem.* **272,** 6663–6670.
36. Hallenberger, S., Bosch, V., Angliker, H., Shaw, E., Klenk, H.-D. & Garten, W. (1992) *Nature (London)* **360,** 358–361.
37. Molloy, S. S., Anderson, E. D., Jean, F. & Thomas, G. (1999) *Trends Cell Biol.* **9,** 28–35.
38. Bravo, D. A., Gleason, J. B., Sanchez, R. I., Roth, R. A. & Fuller, R. S. (1994) *J. Biol. Chem.* **269,** 25830–25837.
39. Wan, L., Molloy, S. S., Thomas, L., Liu, G., Xiang, Y., Rybak, S. L. & Thomas, G. (1998) *Cell* **94,** 205–216.
40. Cole, N. B., Ellenberg, J., Song, J., DiEuliis, D. & Lippincott-Schwartz, J. (1998) *J. Cell Biol.* **140,** 1–14.
41. Kim, S.-H., Wang, R., Gordon, D. J., Bass, J., Steiner, D. F., Lynn, D. G., Thinakaran, G., Meredith, S. C. & Sisodia, S. S. (1999) *Nat. Neurosci.* **2,** 984–988.
42. Bauskin, A. R., Zhang, H. P., Fairlie, W. D., He, X. Y., Russell, P. K., Moore, A. G., Brown, D. A., Stanley, K. K. & Breit, S. N. (2000) *EMBO J.* **19,** 2212–2220.